Detailed characterization of PD-1/PD-L1 and CTLA4 expression and tumor-infiltrating lymphocytes in yolk sac tumors

Hanjie Xu
Huazhong University of Science and Technology
Danya Zhang
Huazhong University of Science and Technology
Can Zhao
Huazhong University of Science and Technology
Lingzhi Qin
Huazhong University of Science and Technology
Rui Wei
Huazhong University of Science and Technology
Ling Xi
Huazhong University of Science and Technology
Fei Li (lifeianhui@163.com)
Huazhong University of Science and Technology

Research Article

Keywords: yolk sac tumors, PD-1, PD-L1, CTLA4, tertiary lymphoid structures

Posted Date: June 22nd, 2022

DOI: https://doi.org/10.21203/rs.3.rs-1765232/v1

Abstract

Background: Immune checkpoint blockade (ICB) is considered as a promising approach for cancer treatment. However, the potency of ICB therapy in yolk sac tumors (YSTs) has not been confirmed, and the comprehensive analysis of tumor immune microenvironment and the expression of PD-1/PD-L1 and CTLA4 were also not thoroughly evaluated.

Methods: Immunohistochemistry was performed in formalin-fixed, paraffin-embedded tumor specimens from 23 YSTs patients to detect the density and distribution of tumor-infiltrating T cells, tertiary lymphoid structures (TLSs), as well as the expression of PD-1/PD-L1 and CTLA4.

Results: Overall, more than half (61%) of all patients exhibited an immune-desert phenotype based on $CD3^+$ T cells. PD-1 expression was identified in five tumor samples (21.7%), and PD-L1 expression exhibited a different positive rate in tumor cells (TCs) and tumor-infiltrating lymphocytes (TILs) (39.1% and 17.4%). Noteworthily, the rate of positive CTLA4 expression in both TCs and TILs was markedly higher (69.6% and 56.5%) than those of PD-1 and PD-L1 expression. Furthermore, TLSs were observed in 21.74% of all tissues, and samples with TLSs exhibited significantly higher densities of TILs and higher expression of immune checkpoint molecules, particularly PD-1/PD-L1. In addition, tumors located in testes also exhibited a higher density of TILs and higher expression of immune checkpoint molecules.

Conclusion: Although a high frequency of CTLA4 expression was found, PD-1/PD-L1 expression, the immune-inflamed phenotype, and TLSs were low frequency in YSTs, suggesting that only a few YSTs patients may be benefit form ICB therapy. Remarkably, patients with tumors located in testes are more likely to benefit from ICB therapy.

Introduction

YSTs are rare malignant germ cell tumors characterized by an extraembryonic yolk sac line of differentiation. Although the majority of patients are cured by surgery and chemotherapy, a subgroup of them have a poor clinical outcome due to chemotherapy resistance, relapse and intolerance of chemotherapy side effects[1, 2]. Therefore, there is an urgent need to discover more effective and less toxic treatments for these patients.

Programmed death receptor 1 (PD-1, CD279), which belongs to the CD28/CTLA4/ICOS costimulatory receptor family, delivers negative signals that impair the immune effects of lymphocytes by combining with programmed death receptor ligand 1 (PD-L1)[3]. Another member of the family, cytotoxic T lymphocyte antigen 4 (CTLA4, CD152), can also suppress the activation of T lymphocytes[4]. Promisingly, inhibition of the interaction of PD-1 and PD-L1 and CTLA4 with its ligands can stimulate T lymphocyte responses and mediate antitumor effects[5, 6]. Based on these encouraging results, immune checkpoint blockade (ICB) agents, which are antibodies blocking PD-1/PD-L1 and CTLA4, have been approved by the US Food and Drug Administration for the treatment of multiple cancer. Up-regulation of immune checkpoint molecules has been be shown to be related to an efficient response to ICB treatment;

nevertheless, only a proportion of people with positive expression of these immune checkpoint molecules exhibit significant clinical responses, indicating that the expression of immune checkpoint molecules is necessary but insufficient for inducing a clinical response [7–9].

Antitumor immunity, regulated through complex factors in the tumor microenvironment (TME), could exhibit distinct responses to ICB therapy[10, 11]. The TME can be grouped in three immune phenotypes based on immune topography: 1) the “immune-desert” phenotype is totally free of infiltrating T cells in both the stroma and inside the tumors; 2) the “immune-excluded” phenotype is characterized by the presence of abundant immune cells in the invasive margin but not inside the tumor; 3) the “immune-inflamed” phenotype is characterized by infiltrating T cells in the tumor parenchyma, which are associated with an antitumor effect[10, 12]. Furthermore, it has been confirmed that different immune phenotypes could create variable immune responses[10, 11].

In addition to both the expression of immune checkpoint molecules and immune phenotypes, the potential influence of tumor-infiltrating B lymphocytes therapeutic response is of growing interest, particularly when these cells are found in relation to organized lymphoid aggregates known as TLSs[13, 14]. Extensive studies have indicated that TLSs play a crucial role in the tumor immune microenvironment, by conferring distinct T cell phenotypes and improving responses to ICB agents, and their presence could be a good predictive biomarker for ICB therapy[15–17].

However, the potency of ICB therapy in YSTs has not been confirmed, for these predictive biomarkers were less well-studied. In this study, the immune phenotypes of tumor-infiltrating T lymphocytes and TLSs and the expression of PD-1/PD-L1 and CTLA4 in YSTs were extensively and deeply assessed to provide a solid basis for ICB therapy.

Materials And Methods

Patients

A total of 23 paraffin-embedded tissue samples from patients diagnosed with YSTs were prospectively obtained from Tongji Hospital (Wuhan, China) between 2017 and 2021. The tissues were retrieved at operation and prior to any therapy. Clinical characteristics, including age at diagnosis and tumor locations and stage were detailed in Table 1. Clinical files and histology data were assessed according to the American Joint Committee on Cancer (AJCC) and the World Health Organization (WHO) classification. The study was approved by the ethics committee of Tongji Hospital of Huazhong University of Science and Technology (identifier: TJ-IRB20210822), and the informed written consent obtained from each patient.

Table 1
Clinical characteristics of 23 diagnosed YST patients

Characteristics		**Number(%)**
Age at diagnosis(years)	**Median** (range)	
	22(1–64)	
Sex		
Female		14(61%)
Male		9(39%)
Subtypes		
Pure		14(61%)
Mixed		
with benign tumor component		4(17%)
with malignant tumor		5(22%)
pT		
T1		9(39%)
T2 ~ 3		11(48%)
Tx		3(13%)
pN		
N0		11(48%)
N1		2(9%)
Nx		10(43%)
pM		
M0		12(52%)
M1		3(13%)
Mx		8(35%)
Location		
Extra-gonad		6(26%)
Gonad		

Characteristics	Number(%)
Ovary	13(57%)
Testicle	4(17%)

Immunohistochemistry and pathological assessment

Hematoxylin-eosin staining and immunohistochemical (IHC) were performed on all samples. The following IHC antibodies were used: anti-CD3 (clone EP41, ZSGB-BIO), anti-CD4 (clone EP204, ZSGB-BIO), anti-CD8 (clone SP16, ZSGB-BIO), anti-Foxp3 (clone 236A/E7, Abcam), anti-CD20 (clone L26, Thermo Fisher Scientific), anti-PD-1 (clone UMAB199, ZSGB-BIO), anti-PD-L1 (clone EPR19759, Abcam), and anti-CTLA4 (clone UMAB249, ZSGB-BIO). The density of lymphocytes in the tumor nest and septa regions was assessed by two examiners as the average in 10 high-power fields with at least 500 cells. TLSs were defined as dense aggregates of B lymphocytes with an adjacent T cell zone[18, 19]. PD-L1 and CTLA4 scores were evaluated separately in tumor cells (TCs) and lymphocytes, and PD-1 scores were assessed in lymphocytes. A 5% cut-off value was performed for PD-1 and PD-L1 positivity based on previous studies of testicular germ cell tumors and ovarian carcinoma[20, 21]. For CTLA4, the staining intensity was scored as follows: negative, 0; weak, 1; moderate, 2; and strong, 3. The percentage of positive cells was also scored as follows: 0 (< 10% positive cells), 1 (10–30% positive cells), 2 (31–50% positive cells), and 3(> 50% positive cells). The sum of the scores for staining intensity and percentage of positive cells was the staining score, which was divided into negative (score ≤ 1) and positive expression (score > 2) [22].

Statistics

Statistical analyses were performed in the R software environment (version 4.1.2). The “ggpubr” R package (https://mirror.lzu.edu.cn/CRAN/bin/windows/contrib/4.1/ggpubr_0.4.0.zip) was used to perform statistical analysis. Comparisons between more than two groups were made using the Kruskal-Wallis test, and comparisons between two groups were made using the Wilcox test. A *P* value less than 0.05 was considered significant.

Results

Baseline characteristics

The clinical and pathological characteristics of the 23 YSTs patients are described in Table 1. The mean age of the patients was 22 years (range 1–64 years). Nine patients were male (39%) and 14 were female (61%). The histopathological evaluation showed that 61% of tumors were pure YSTs, 17% were mixed with benign tumors, and 22% were mixed with malignant tumors. The pT, pN, and pM of the YSTs are also detailed in Table 1. Additionally, the most frequent primary tumor location was the ovaries, followed by extragonadal sites.

Density and spatial distribution of tumor-infiltrating T lymphocytes

The density and pattern of lymphocyte distribution demonstrated that tumor-infiltrating T lymphocytes were scattered in the tumor nests with denser aggregates located in septa regions, illustrating that samples ranged in phenotype from an immune-inflamed phenotype to an immune-desert phenotype (Figs. 1A, S1). More than half of all samples (61%) exhibited the immune-desert phenotype, while 26% of samples showed the immune-inflamed phenotype, and 13% showed the immune-excluded phenotype (Fig. 1B). Tumors located in testes had more infiltrated $CD3^+$ T cells than those located in either ovaries or extragonadal sites (Fig. 1C). The immune-inflamed phenotype was obviously most common among all four cases with tumors located in testes, whereas the immune-desert phenotype was found in the majority of the tumors located in extragonadal sites (66%) and ovaries (77%) (Fig. 1D).

The majority (69% and 78%, respectively) of samples displayed the immune-desert phenotype based on the density and spatial distribution of $CD4^+$ and $CD8^+$ T cells, while the others displayed the immune-inflamed phenotype (22%, 18%) or immune-excluded phenotype (9%, 4%) (Fig. 1B). Tumor-infiltrating $Foxp3^+$ T cells were observed in samples redundantly infiltrated by $CD3^+$, $CD4^+$ and $CD8^+$ T cells, but the density was much lower than that of the other T cell subsets (Figs. 1A, S1). With respect to the $Foxp3^+$ T cell immune phenotype, two cases (9%), three cases (13%) and 18 cases (78%) showed the immune-inflamed phenotype, immune-excluded phenotype, and immune-desert phenotype, respectively (Fig. 1B).

Immune checkpoints expression: PD-1/PD-L1 and CTLA4

Typical staining of PD-1 was detected in lymphocytes, which were located in tumor nests and septa regions (Fig. 2B). The rate of positive PD-1 expression was 21.74% (5/23). PD-L1 expression in TILs ($PD\text{-}L1_L$) was identified in four tumor samples (17.4%), and its expression in TCs ($PD\text{-}L1_T$) was found in nine specimens (39.13%). Higher expression of CTLA4 than of PD-1 and PD-L1 was found; positive expression was detected in TILs ($CTLA4_L$) in 13 specimens, and 16 specimens exhibited positive staining in TCs ($CTLA4_T$), as shown in Fig. 2A.

Further studies of the relationship between immune checkpoint molecules and tumor location found that PD-1 was predominantly expressed in the testes, but at lower levels in both the ovaries and extragonadal sites. The rate of positive $PD\text{-}L1_T$ and/or $PD\text{-}L1_L$ arranged from high to low was as follows: testes, extragonadal sites and ovaries (Fig. 2B). Significantly, all four tumors located in testes had positive $PD\text{-}L1_T$, and two tumors had positive $PD\text{-}L1_L$ expressions. The expression of CTLA4 was also separately evaluated according to tumor site. $CTLA4_T$ staining in testes, extragonadal sites, and ovaries was detected in 100% (4/4), 66.67% (4/6), and 61.54% (8/13) of samples, respectively (Fig. 2B). Interestingly, the rate of positive $CTLA4_L$ for testes was highest, as it was only 33.33% (2/6) for extragonadal sites, and 53.85% for the ovaries (7/13) (Fig. 2B).

Density of B cells and TLSs

$CD20^+$ B cells, which frequently aggregate into TLSs, were identified in 34.78% of the samples (Fig. 3A). To provide more accurate estimates of the density of $CD20^+$ B cells, the numbers of TLSs and the scattered remaining B cells were identified separately. Similar to the organization of T cells, the IHC analyses showed that few scattered B cells were located in tumor nests (denoted as positive $CD20_N$) with more intensive aggregates in tumor septa regions (denoted as positive $CD20_S$), and the differences were statistically significant ($P < 0.05$) (Figure S2).

TLSs were found in 21.74% of all tissues with a median of 3.48 TLSs per cm^2 of tissue specimens among the TLS^+ tumors. Interestingly, heatmap analysis revealed that most samples with TLSs had a similar immune phenotype: a higher density of T cells and positive expression of PD-1, PD-L1, and CTLA4 (Fig. 3D). Quantitatively, samples with TLSs exhibited significantly higher densities of tumor-infiltrating T lymphocytes than those with no TLSs, but the differences in CD8 expression did not reach statistical significance (Fig. 3C). Additionally, mirroring the tumor-infiltrating T lymphocyte data, samples with positive expression of PD-1 and PD-L1 had a higher proportion of TLSs; however, a higher proportion of TLSs was not found in tumors with $CTLA4_T^+$ and $CTLA4_L^+$ (Fig. 3C). Consistent with the above results, various immune cells were detected in the same TLS, including $CD4^+$, $CD8^+$ and $Foxp3^+$ T cells, $PD\text{-}1^+$ cells, $PD\text{-}L1^+$ cells, and $CTLA4^+$ cells (Figure S3).

The association between TILs and immune checkpoint molecules: PD-1, PD-L1 and CTLA4

The prevalence of positive PD-1/PD-L1 and CTLA4 expression and its potential correlation with TIL density were assessed. The findings indicated that $PD\text{-}1^+$ tumors exhibited a higher density of TILs ($CD3^+$, $CD4^+$, and $Foxp3^+$ T cells and $CD20^+$ B cells) in the nests or septa regions of tumors than $PD\text{-}1^-$ tissues. A higher density of tumor-infiltrating $CD8^+$ T lymphocytes was also found in $PD\text{-}1^+$ tumors, but the difference failed to reach statistical significance ($P = 0.10$ for $CD8_N$ and $P = 0.05$ for $CD8_S$) (Fig. 4A). Furthermore, there was a substantial difference in the composition of TILs between tumors positive and negative PD-L1 expression. In contrast to $PD\text{-}L1_T^-$ tumors, $PD\text{-}L1_T^+$ tumors had a higher density of TILs, and the differences were statistically significant, except for those for $CD4_N$, $CD20_N$ and $CD20_S$. Similar results were also found in tumors with positive $PD\text{-}L1_L^+$ (Fig. 4B). Statistical analyses of the composition of TILs between the $CTLA4^+$ and $CTLA4^-$ groups were also performed. A higher TILs density was found in $CTLA4_L^+$ tumors than in the $CTLA4_L^-$ tumors; however, only the differences in the infiltration of $CD3^+$, $CD4_S^+$ and $CD8_S^+$ T cells were statistically significant ($P < 0.05$) (Fig. 4C). In general, these results showed that the expression of immune checkpoint molecules, particularly PD-1/PD-L1, was associated with a higher TIL density, indicating that these tumors may be sensitive to ICBs.

Discussion

With respect to research of ICB therapy YSTs was few, and was often included in the study of testicular germ cell tumors. This study is the first comprehensive and detailed assessment of PD-1/PD-L1 and CTLA4 expression and tumor-infiltrating lymphocytes for evaluating the potency of ICB therapy in YSTs. Remarkably, the presence and frequency of TLSs in YSTs were also first reported in the study. The observed results demonstrated that only a small proportion of patients, which had tumor-infiltrating lymphocytes and the expression of immune checkpoint molecules present, may be efficacious for ICB agents.

That the expression levels of PD-1/PD-L1 and CTLA4 are significant predictive biomarkers in cancer immunotherapy, has already been confirmed by extensive studies[23–25]. The expression of CTLA4 has been almost exclusively studied in the TILs, but increasing evidence has shown its expression on tumors with clinical response to ICB therapy. Notably, a high frequency of both $CTLA4_T^+$ and $CTLA4_L^+$ was found in our study, suggesting that anti-CTLA4 targeted therapy may be improve the prognosis of YSTs patients. However, this idea should be applied with caution, as until now, CTLA4 expression in YSTs has rarely been reported in the published literature[26]. Also, the existence of patients with negative expression and positive responses has been previously reported and confirmed that the expression of CTLA4 is not an adequate biomarker to select candidate patients for ICB[27]. The results by Hamid et al revealed significant associations between positive response and high baseline expression of Foxp3, and between positive response and increase in TILs between baseline and 3 weeks after start of treatment[28]. In addition, Mastracci et al also demonstrated that high TIL score and density of $CD3^+$, $CD8^+$ T cells, and $CTLA4_L^+$ were significantly associated with a better response to anti-CTLA4 targeted therapy in patients with melanoma[29]. These results suggested that the expression of $CTLA4^+$ ($CTLA4_T^+$ or $CTLA4_L^+$) in combination with TILs may be optimal marker for selecting patients who could be candidates for anti-CTLA4 therapy. In our study, although a high frequency of both $CTLA4_T^+$ and $CTLA4_L^+$ was found; only a small subset of patients exhibited the immune-inflamed phenotype or with TLSs, suggesting that anti-CTLA4 therapy is not optimal choice for most YSTs patients.

In our study, five patients (21.74%) had positive PD-1 expression, indicating that YSTs exhibited a low frequency of PD-1 expression. As to PD-L1, that $PD\text{-}L1_T$ and $PD\text{-}L1_L$ had different prognostic values highlighted the importance of separately evaluating their expression[30]. Nevertheless, the study of PD-L1 not only was few in YSTs, but also has been assessed without distinguishing between TCs and lymphocytes in the most studies. In our study, the $PD\text{-}L1_T$ and $PD\text{-}L1_L$ were observed, and the results showed that nine cases (39.1%) had positive $PD\text{-}L1_T$, and four cases (17.4%) had positive $PD\text{-}L1_L$. Fankhauser et al found that 19 (40%) patients with YSTs exhibited positive expression of PD-L1 without distinguishing between TCs and lymphocytes, the results were consistent with the expression with $PD\text{-}L1_T$ in our study[20]. Consistent with our study, one study showed that five of 26 patients exhibited positive $PD\text{-}L1_L$, and another study found that no positive expression was detected in four YST patients[30, 31]. These results demonstrated that the frequency of $PD\text{-}L1_L$ expression was low in YSTs.

The up-regulation of immune checkpoint molecules has been associated with an effective clinical response to ICB treatment; however, recent studies indicate that tumor-infiltrating lymphocytes is also crucial to positive responses[29, 32, 33]. In the study, we found that the immune-desert phenotype prevailed among YSTs, while only a minority exhibited the immune-inflamed phenotype. The immune-excluded phenotype featured massive infiltration of immune cells; however, the immune cells do not penetrate the parenchyma and instead are present tumor septa regions[10]. The septa impose restrictions on the killing activity of T cells in response to TCs. Hence, with anti-PD-1/PD-L1 agent treatment, tumor-infiltrating T cells in tumors of the immune-excluded phenotype can demonstrate evidence of activation and proliferation but not infiltration, and thus, responses are likely to be uncommon[10]. Due to the paucity of T cells in both the nest and septa regions of the tumor, the immune-desert phenotype represents a non-inflamed TME. Unsurprisingly, these tumors rarely respond to anti-PD-L1/PD-1 immunotherapy[33].

In Boldrini's research, among 28 YST cases, more than half of the cases featured the immune-desert phenotype, and 39% of the cases featured the immune-inflamed phenotype, consistent with our results[34]. Compared with that study, we further assessed TLSs, that are involved in the TILs and contribute to ICB therapy response[13, 35]. To date, no assessment of TLSs in YSTs has been reported. In our study, five patients had TLSs, and the composition of TLSs was also assessed. Strikingly, multiple immune cells were present in the TLSs, including $CD4^+$, $CD8^+$ and $Foxp3^+$ T cells, $PD\text{-}1^+$ cells, $PD\text{-}L1^+$ cells, and $CTLA4^+$ cells. We further analyzed the relationship of TLSs with both TILs and the expression of PD-1/PD-L1 and CTLA4. The density of TILs and the expression of PD-1/PD-L1 were higher in patients with TLSs than in those without TLSs. The above results illustrated that TLSs have a key role in the immune microenvironment and may improve responses to ICB therapy in YSTs.

Due to both the density of TILs and the immune checkpoint molecules expression were strongly associated with the response to ICB therapy, their relations were also explored in our study. Consistent with another study, the expression of PD-1 was proportional to the density of TILs in the study[34]. However, the differences in tumor-infiltrating $CD8^+$ T cells failed to reach statistical significance (P = 0.1024 for $CD8_N$ and P = 0.0519 for $CD8_S$), likely due to the small sample sizes. Similar to the results for PD-1, a higher density of TILs was also found in patients with PD-L1 positivity. In addition, we also found a higher density of TILs in patients with positive $CTLA4_L$; nonetheless, no association was demonstrated between $CTLA4_T$ and the density of TILs.

Interestingly, we found that compared with tumors located in extragonadal sites or the ovaries, YSTs located in the testes usually have an exceptionally higher TLSs and expression of PD-1/PD-L1 and CTLA4, as well as more tumor-infiltrating T cells. The results suggested that YSTs located in the testes could profit from immunotherapeutic strategies using ICB, but a larger sample size is needed to confirm this finding.

We identified the immune phenotype of tumor-infiltrating T cells, a low frequency of PD-1/PD-L1 expression, a high frequency of CTLA4 expression, the presence of TLSs and relationships between these

factors in YSTs. These features indicated that only a few YSTs patients may be benefit form ICB therapy; alternatively, converting the tumor from “cold” to “hot” could be a useful strategy prior to immunotherapy for most patients. A major limitation of our study might be the lack of neoadjuvant ICB trial data. Nevertheless, our comprehensive and detailed description of PD-1/PD-L1 and CTLA4 expression and tumor-infiltrating lymphocytes in YSTs forms a solid basis for ICB therapy.

In conclusion, ICB therapy could be a promising new treatment approach in YSTs, however, only a few YSTs patients may be benefit from these, and assessing TILs and the expression of immune checkpoint molecules for stratification is an indispensable part. Excitingly, patients with tumors located in testes exhibited a higher density of TILs and higher expression of immune checkpoint molecules, and might be efficacious for ICB therapy.

Declarations

Acknowledgements

The authors would like to acknowledge the pathology department of Tongji Hospital in the technical support.

Funding

This work was supported by the National Natural Science Foundation of China (81802608, 82002764).

Availability of data and materials

The raw data are available upon request on the following e-mail address: lifeianhui@163.com.

Authors’ contributions

The study was proposed and designed by LX and FL. HX, DZ, and CZ performed the experiments. Data collection and analysis were performed by LQ and RW. The manuscript was drafted by HX and checked by LX and FL. All authors read and approved the final manuscript.

Ethics approval and consent to participate

The study was approved by the ethics committee of Tongji Hospital of Huazhong University of Science and Technology (identifier: TJ-IRB20210822). The informed written consent obtained from each patient.

Consent for publication

Not applicable.

Competing interests

The authors declare that they have no known competing financial interests or personal relationships that could have appeared to influence the work reported in this paper.

References

1. Brown J, Friedlander M, Backes FJ, Harter P, O'Connor DM, de la Motte Rouge T, Lorusso D, Maenpaa J, Kim JW, Tenney ME *et al*: Gynecologic Cancer Intergroup (GCIG) consensus review for ovarian germ cell tumors. Int J Gynecol Cancer 2014, 24(9 Suppl 3):S48-54.
2. Dallenbach P, Bonnefoi H, Pelte MF, Vlastos G: Yolk sac tumours of the ovary: an update. Eur J Surg Oncol 2006, 32(10):1063–1075.
3. Zhang X, Schwartz JC, Guo X, Bhatia S, Cao E, Lorenz M, Cammer M, Chen L, Zhang ZY, Edidin MA *et al*: Structural and functional analysis of the costimulatory receptor programmed death-1. Immunity 2004, 20(3):337–347.
4. Rowshanravan B, Halliday N, Sansom DM: CTLA-4: a moving target in immunotherapy. Blood 2018, 131(1):58–67.
5. Rudqvist NP, Pilones KA, Lhuillier C, Wennerberg E, Sidhom JW, Emerson RO, Robins HS, Schneck J, Formenti SC, Demaria S: Radiotherapy and CTLA-4 Blockade Shape the TCR Repertoire of Tumor-Infiltrating T Cells. Cancer Immunol Res 2018, 6(2):139–150.
6. Berger R, Rotem-Yehudar R, Slama G, Landes S, Kneller A, Leiba M, Koren-Michowitz M, Shimoni A, Nagler A: Phase I safety and pharmacokinetic study of CT-011, a humanized antibody interacting with PD-1, in patients with advanced hematologic malignancies. Clin Cancer Res 2008, 14(10):3044–3051.
7. Robert C, Ribas A, Wolchok JD, Hodi FS, Hamid O, Kefford R, Weber JS, Joshua AM, Hwu WJ, Gangadhar TC *et al*: Anti-programmed-death-receptor-1 treatment with pembrolizumab in ipilimumab-refractory advanced melanoma: a randomised dose-comparison cohort of a phase 1 trial. Lancet 2014, 384(9948):1109–1117.
8. Rexer H, Bergmann L, Steiner T: [A Phase 2, Randomized, Open-Label Study of Nivolumab Combined with Ipilimumab Versus Sunitinib Monotherapy in Subjects with Previously Untreated and Advanced (unresectable or metastatic) non-clear Cell Renal Cell Carcinoma - SUNNIFORECAST AN 41/16 der AUO]. Aktuelle Urol 2020, 51(3):236–238.
9. Valsecchi ME: Combined Nivolumab and Ipilimumab or Monotherapy in Untreated Melanoma. N Engl J Med 2015, 373(13):1270.
10. Chen DS, Mellman I: Elements of cancer immunity and the cancer-immune set point. Nature 2017, 541(7637):321–330.
11. Tumeh PC, Harview CL, Yearley JH, Shintaku IP, Taylor EJ, Robert L, Chmielowski B, Spasic M, Henry G, Ciobanu V *et al*: PD-1 blockade induces responses by inhibiting adaptive immune resistance. Nature 2014, 515(7528):568–571.

12. Hegde PS, Karanikas V, Evers S: The Where, the When, and the How of Immune Monitoring for Cancer Immunotherapies in the Era of Checkpoint Inhibition. Clin Cancer Res 2016, 22(8):1865–1874.
13. Helmink BA, Reddy SM, Gao J, Zhang S, Basar R, Thakur R, Yizhak K, Sade-Feldman M, Blando J, Han G *et al*: B cells and tertiary lymphoid structures promote immunotherapy response. Nature 2020, 577(7791):549–555.
14. Meshcheryakova A, Tamandl D, Bajna E, Stift J, Mittlboeck M, Svoboda M, Heiden D, Stremitzer S, Jensen-Jarolim E, Grunberger T *et al*: B cells and ectopic follicular structures: novel players in anti-tumor programming with prognostic power for patients with metastatic colorectal cancer. PLoS One 2014, 9(6):e99008.
15. Cabrita R, Lauss M, Sanna A, Donia M, Skaarup Larsen M, Mitra S, Johansson I, Phung B, Harbst K, Vallon-Christersson J *et al*: Tertiary lymphoid structures improve immunotherapy and survival in melanoma. Nature 2020, 577(7791):561–565.
16. Gide TN, Quek C, Menzies AM, Tasker AT, Shang P, Holst J, Madore J, Lim SY, Velickovic R, Wongchenko M *et al*: Distinct Immune Cell Populations Define Response to Anti-PD-1 Monotherapy and Anti-PD-1/Anti-CTLA-4 Combined Therapy. Cancer Cell 2019, 35(2):238–255 e236.
17. Riaz N, Havel JJ, Makarov V, Desrichard A, Urba WJ, Sims JS, Hodi FS, Martin-Algarra S, Mandal R, Sharfman WH *et al*: Tumor and Microenvironment Evolution during Immunotherapy with Nivolumab. Cell 2017, 171(4):934–949 e916.
18. Germain C, Gnjatic S, Tamzalit F, Knockaert S, Remark R, Goc J, Lepelley A, Becht E, Katsahian S, Bizouard G *et al*: Presence of B cells in tertiary lymphoid structures is associated with a protective immunity in patients with lung cancer. Am J Respir Crit Care Med 2014, 189(7):832–844.
19. Sautes-Fridman C, Petitprez F, Calderaro J, Fridman WH: Tertiary lymphoid structures in the era of cancer immunotherapy. Nat Rev Cancer 2019, 19(6):307–325.
20. Fankhauser CD, Curioni-Fontecedro A, Allmann V, Beyer J, Tischler V, Sulser T, Moch H, Bode PK: Frequent PD-L1 expression in testicular germ cell tumors. Br J Cancer 2015, 113(3):411–413.
21. Buderath P, Mairinger F, Mairinger E, Bohm K, Mach P, Schmid KW, Kimmig R, Kasimir-Bauer S, Bankfalvi A, Westerwick D *et al*: Prognostic significance of PD-1 and PD-L1 positive tumor-infiltrating immune cells in ovarian carcinoma. Int J Gynecol Cancer 2019, 29(9):1389–1395.
22. You H, Zhang YZ, Lai HL, Li D, Liu YQ, Li RZ, Khan I, Hsiao WW, Duan FG, Fan XX *et al*: Prognostic significance of tumor poliovirus receptor and CTLA4 expression in patients with surgically resected non-small-cell lung cancer. J Cancer Res Clin Oncol 2020, 146(6):1441–1450.
23. Zouein J, Kesrouani C, Kourie HR: PD-L1 expression as a predictive biomarker for immune checkpoint inhibitors: between a dream and a nightmare. Immunotherapy 2021, 13(12):1053–1065.
24. Pico de Coana Y, Wolodarski M, van der Haar Avila I, Nakajima T, Rentouli S, Lundqvist A, Masucci G, Hansson J, Kiessling R: PD-1 checkpoint blockade in advanced melanoma patients: NK cells, monocytic subsets and host PD-L1 expression as predictive biomarker candidates. Oncoimmunology 2020, 9(1):1786888.

25. Pistillo MP, Fontana V, Morabito A, Dozin B, Laurent S, Carosio R, Banelli B, Ferrero F, Spano L, Tanda E *et al*: Soluble CTLA-4 as a favorable predictive biomarker in metastatic melanoma patients treated with ipilimumab: an Italian melanoma intergroup study. Cancer Immunol Immunother 2019, 68(1):97–107.
26. Lobo J, Rodrigues A, Guimaraes R, Cantante M, Lopes P, Mauricio J, Oliveira J, Jeronimo C, Henrique R: Detailed Characterization of Immune Cell Infiltrate and Expression of Immune Checkpoint Molecules PD-L1/CTLA-4 and MMR Proteins in Testicular Germ Cell Tumors Disclose Novel Disease Biomarkers. Cancers (Basel) 2019, 11(10).
27. Santos-Briz A, Canueto J, Carmen SD, Barrios B, Yuste M, Bellido L, Ludena MD, Roman C: Value of PD-L1, PD-1, and CTLA-4 Expression in the Clinical Practice as Predictors of Response to Nivolumab and Ipilimumab in Monotherapy in Patients With Advanced Stage Melanoma. Am J Dermatopathol 2021, 43(6):423–428.
28. Hamid O, Schmidt H, Nissan A, Ridolfi L, Aamdal S, Hansson J, Guida M, Hyams DM, Gomez H, Bastholt L *et al*: A prospective phase II trial exploring the association between tumor microenvironment biomarkers and clinical activity of ipilimumab in advanced melanoma. J Transl Med 2011, 9:204.
29. Mastracci L, Fontana V, Queirolo P, Carosio R, Grillo F, Morabito A, Banelli B, Tanda E, Boutros A, Dozin B *et al*: Response to ipilimumab therapy in metastatic melanoma patients: potential relevance of CTLA-4(+) tumor infiltrating lymphocytes and their in situ localization. Cancer Immunol Immunother 2020, 69(4):653–662.
30. Chovanec M, Cierna Z, Miskovska V, Machalekova K, Svetlovska D, Kalavska K, Rejlekova K, Spanik S, Kajo K, Babal P *et al*: Prognostic role of programmed-death ligand 1 (PD-L1) expressing tumor infiltrating lymphocytes in testicular germ cell tumors. Oncotarget 2017, 8(13):21794–21805.
31. Aoki T, Hino M, Koh K, Kyushiki M, Kishimoto H, Arakawa Y, Hanada R, Kawashima H, Kurihara J, Shimojo N *et al*: Low Frequency of Programmed Death Ligand 1 Expression in Pediatric Cancers. Pediatr Blood Cancer 2016, 63(8):1461–1464.
32. Topalian SL, Hodi FS, Brahmer JR, Gettinger SN, Smith DC, McDermott DF, Powderly JD, Carvajal RD, Sosman JA, Atkins MB *et al*: Safety, activity, and immune correlates of anti-PD-1 antibody in cancer. N Engl J Med 2012, 366(26):2443–2454.
33. Herbst RS, Soria JC, Kowanetz M, Fine GD, Hamid O, Gordon MS, Sosman JA, McDermott DF, Powderly JD, Gettinger SN *et al*: Predictive correlates of response to the anti-PD-L1 antibody MPDL3280A in cancer patients. Nature 2014, 515(7528):563–567.
34. Boldrini R, De Pasquale MD, Melaiu O, Chierici M, Jurman G, Benedetti MC, Salfi NC, Castellano A, Collini P, Furlanello C *et al*: Tumor-infiltrating T cells and PD-L1 expression in childhood malignant extracranial germ-cell tumors. Oncoimmunology 2019, 8(2):e1542245.
35. Tsou P, Katayama H, Ostrin EJ, Hanash SM: The Emerging Role of B Cells in Tumor Immunity. Cancer Res 2016, 76(19):5597–5601.

Figures

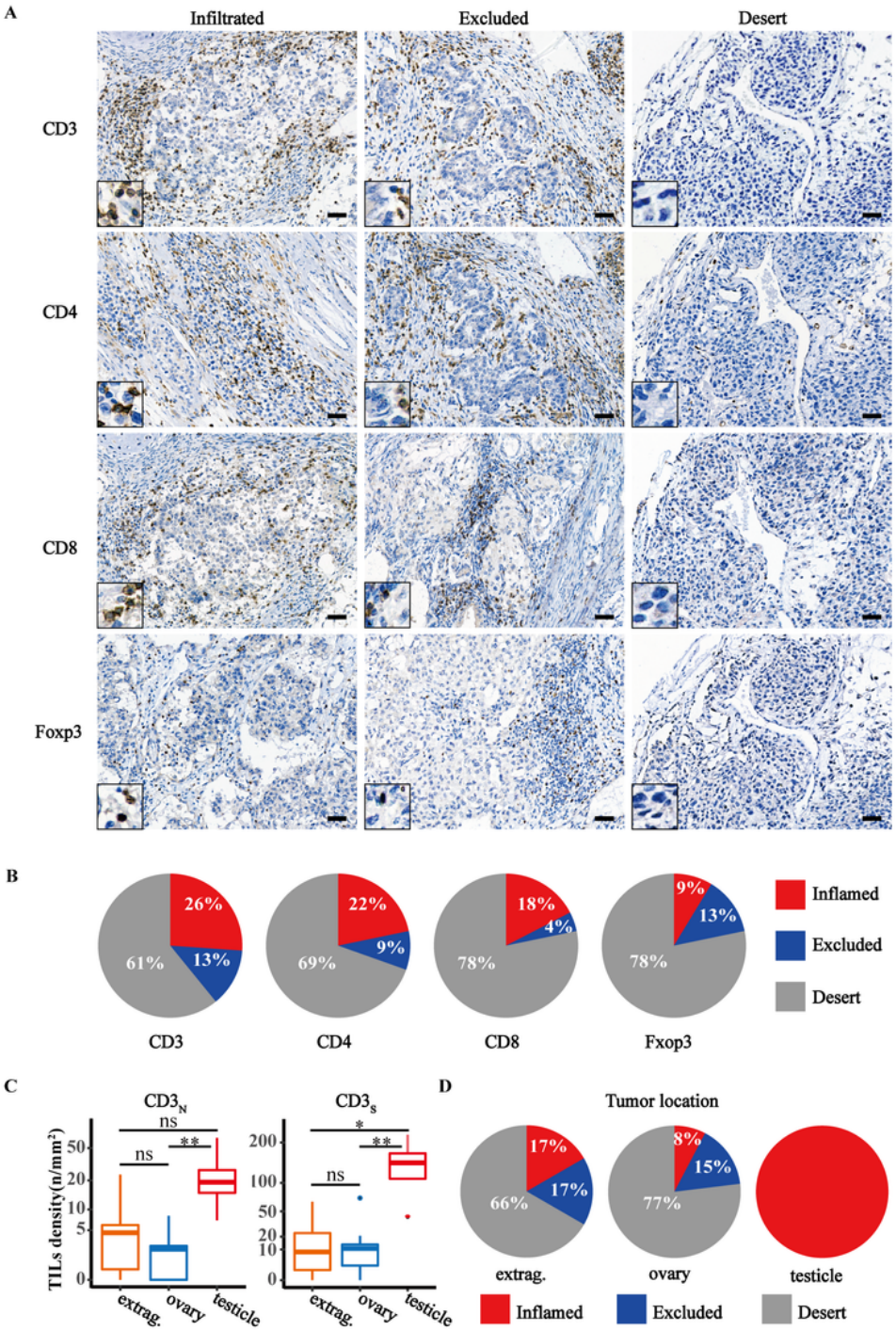

Figure 1. Density and distribution of tumor-infiltrating T lymphocytes in YSTs. **A,** Representative immunohistochemistry images of YST samples with immune-inflamed, immune-excluded and immune-desert phenotypes were shown. Scale bar, 50 μm. **B**, Distribution of tumor-infiltrating T lymphocytes. **C,** Box plot of the tumor-infiltrating CD3+ T cell density in the nest(N) and septa(S) regions of tumors according to tumor location. **D,** Distribution of tumor-infiltrating CD3+ T cells according to tumor location. YSTs: yolk sac tumors; ns: not significant, $P > 0.05$; *: $P < 0.05$; **: $P < 0.01$.

Figure 1

Legend not included with this version.

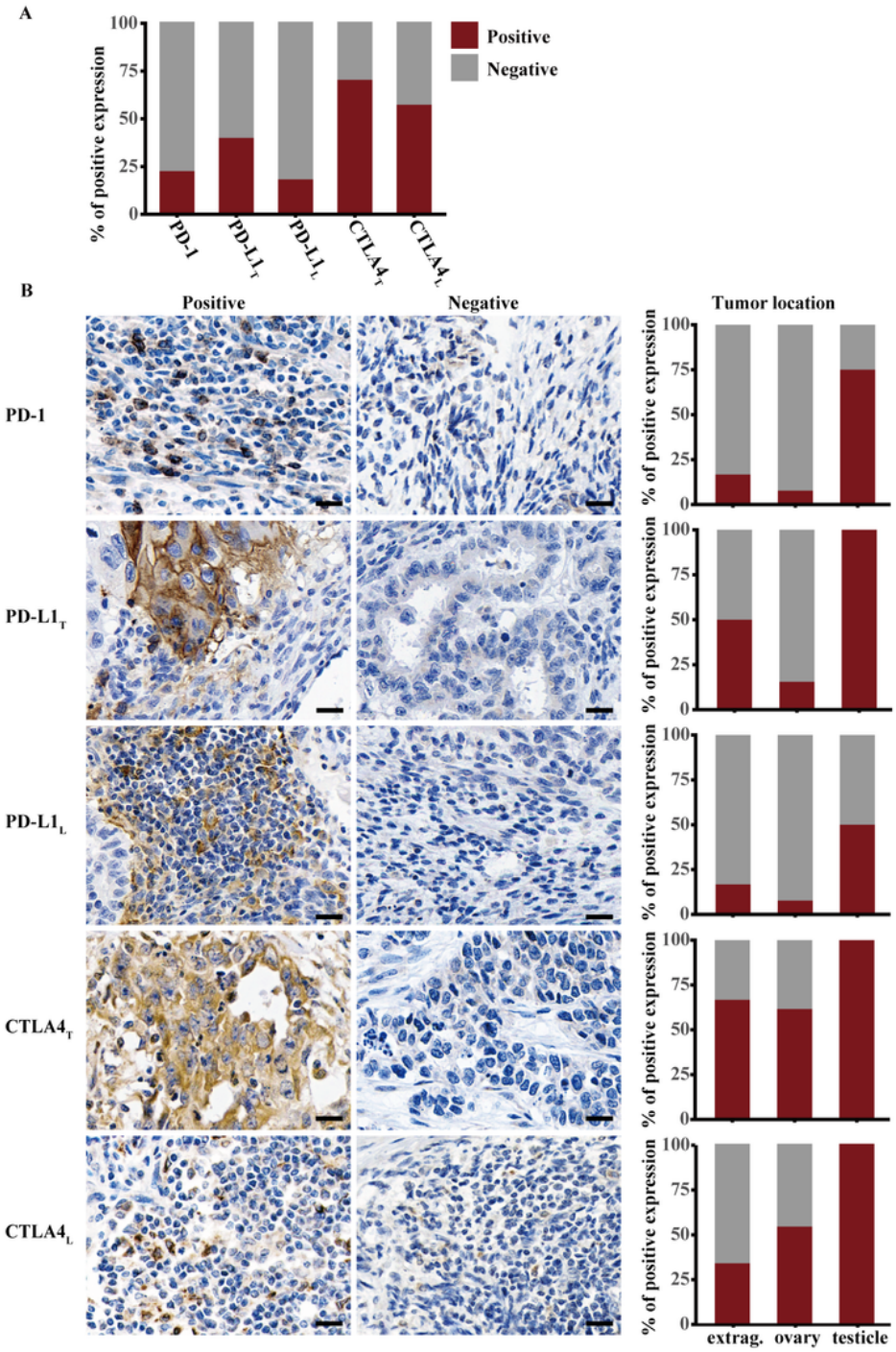

Figure 2. The expression of PD-1/PD-L1 and CTLA4 in YSTs. **A**, The frequency of PD-1/PD-L1 and CTLA4 expression. **B**, Examples illustrating distribution of PD-1/PD-L1 and CTLA4 staining in YSTs. Left panel: representative IHC images for PD-1/PD-L1 and CTLA4 staining; middle panel: representative IHC images for samples with no expression of target molecules; right panel: distribution of target molecule staining in YST patients according to tumor location. Scale bar, 20μm. T: expression in tumor cells; L: expression in lymphocytes.

Figure 2

Legend not included with this version.

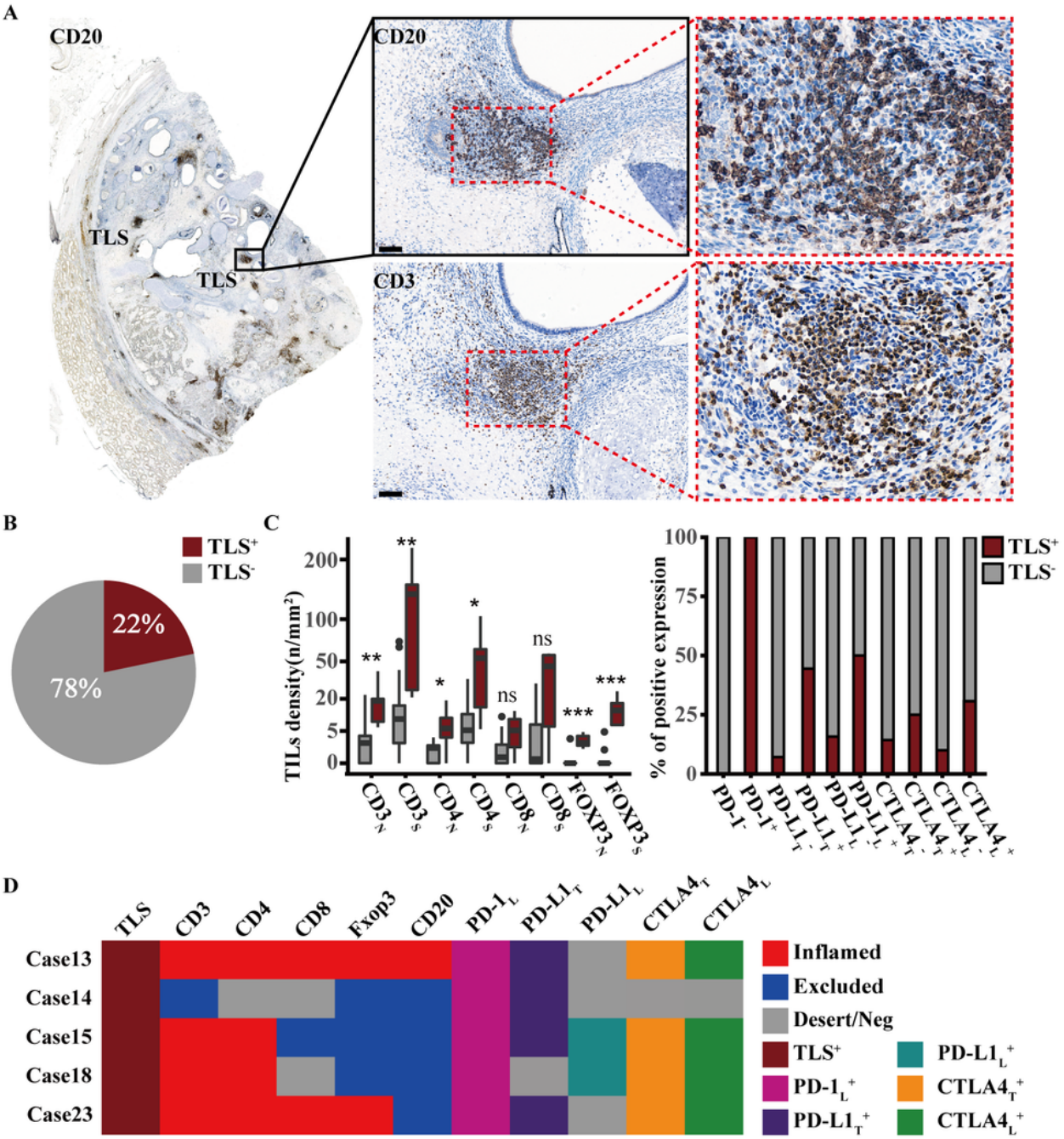

Figure 3. Characterization and distribution of TLSs in YSTs. **A,** Representative IHC images of TLSs. Scale bar, 100 μm. **B,** Frequency of TLSs. **C,** Characterization of TILs and PD-1/PD-L1 and CTLA4 expression according to TLS presence in YSTs. **D,** Distribution of tumor-infiltrating T cell subsets, CD20+ B cells, and PD-1/PD-L1 and CTLA4 expression in YST patients with TLSs. T: expression in tumor cells; L: expression in lymphocytes, N: TILs in the tumor nest, S: TILs in the tumor septa. ns: not significant, $P > 0.05$; *: $P < 0.05$; **: $P < 0.01$.

Figure 3

Legend not included with this version.

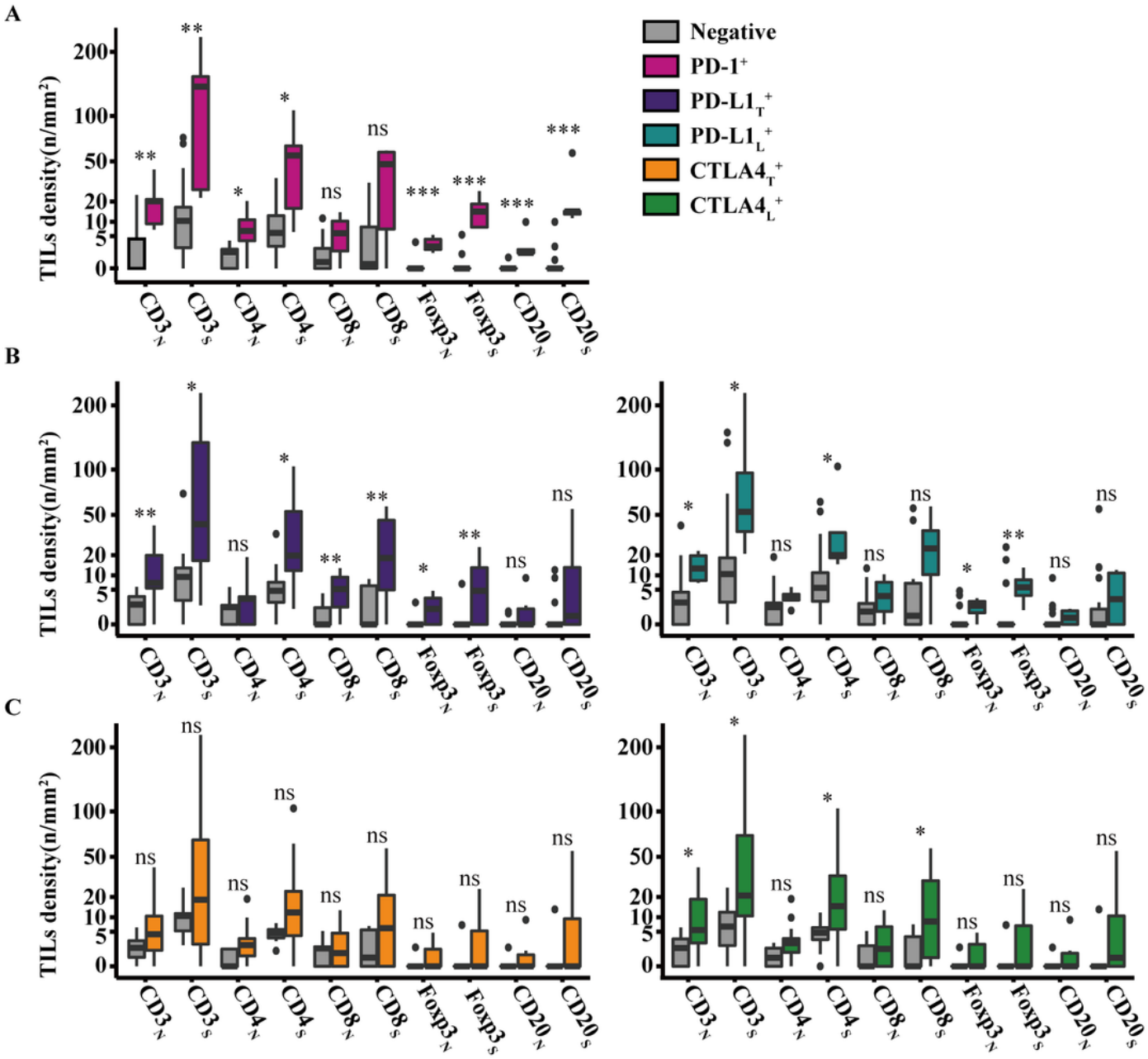

Figure 4. Density of TILs in YSTs according to the expression of PD-1/PD-L1 and CTLA4. **A,** Box plots of tumor-infiltrating T cell subsets and CD20+ B cells according to the expression of PD-1. **B,** Box plots of tumor-infiltrating T cell subsets and CD20+ B cells according to the expression of PD-L1. Left: PD-L1T; right: PD-L1L. **C,** Box plots of tumor-infiltrating T cell subsets and CD20+ B cells according to the expression of CTLA4. Left: CTLA4T; right: CTLA4L. T: expression in tumor cells; L: expression in lymphocytes. N: TILs in the tumor nest, S: TILs in tumor septa. ns: not significant, $P > 0.05$; *: $P < 0.05$; **: $P < 0.01$; ***: $P < 0.001$.

Figure 4

Legend not included with this version.

Supplementary Files

This is a list of supplementary files associated with this preprint. Click to download.

- figsupplement.tif